The First Structure of UDP-Glucose Dehydrogenase Reveals the Catalytic Residues Necessary for the Two-fold Oxidation[†,‡]

Robert E. Campbell,[§] Steven C. Mosimann,[||] Ivo van de Rijn,[⊥] Martin E. Tanner,[§] and Natalie C. J. Strynadka*[,||]

Department of Biochemistry and Molecular Biology, University of British Columbia, Vancouver, British Columbia, Canada V6T 1Z3, Department of Chemistry, University of British Columbia, Vancouver, British Columbia, Canada V6T 1Z1, and Wake Forest University Medical Center, Winston-Salem, North Carolina 27157

Received January 31, 2000; Revised Manuscript Received April 4, 2000

ABSTRACT: Bacterial UDP-glucose dehydrogenase (UDPGlcDH) is essential for formation of the antiphagocytic capsule that protects many virulent bacteria such as *Streptococcus pyogenes* and *Streptococcus pneumoniae* type 3 from the host's immune system. We have determined the X-ray structures of both native and Cys260Ser UDPGlcDH from *S. pyogenes* (74% similarity to *S. pneumoniae*) in ternary complexes with UDP-xylose/NAD^+ and UDP-glucuronic acid/NAD(H), respectively. The 402 residue homodimeric UDPGlcDH is composed of an N-terminal NAD^+ dinucleotide binding domain and a C-terminal UDP-sugar binding domain connected by a long (48 Å) central α-helix. The first 290 residues of UDPGlcDH share structural homology with 6-phosphogluconate dehydrogenase, including conservation of an active site lysine and asparagine that are implicated in the enzyme mechanism. Also proposed to participate in the catalytic mechanism are a threonine and a glutamate that hydrogen bond to a conserved active site water molecule suitably positioned for general acid/base catalysis.

UDP-glucose dehydrogenase (UDPGlcDH)[1] catalyzes the NAD^+-dependent oxidation of UDP-glucose to UDP-glucuronic acid (UDPGlcA) (*1*). Since the original report of this enzymatic activity in preparations of calf liver more than 40 years ago (*2*), UDPGlcDH has been identified in many other sources, and recently the human enzyme has been cloned and sequenced (*3*). The product of UDPGlcDH, UDPGlcA, is the activated donor of the glucuronic acid moiety and serves many critical roles in a variety of organisms ranging from mammals to bacteria. In mammals, UDPGlcA is the substrate for UDP-glucuronosyl transferases in the liver that catalyze the formation of glucuronide conjugates with various substances such as bilirubin and thereby aid in their excretion (*4*). UDPGlcA is also essential for the biosynthesis of hyaluronan and various glycosaminoglycans such as chondroitin sulfate and heparan sulfate (*5*). Mutation of the UDPGlcDH gene of *Drosophilia melanogaster* (designated *sugarless*) disrupts biosynthesis of the heparan sulfate side chains on proteoglycan core proteins and is identical in phenotype to the classical *wingless* mutation (*6*). In plants, UDPGlcDH may be an important regulatory enzyme in the carbon flux toward cell wall and glycoprotein biosynthesis due to feedback inhibition from UDP-xylose (*7*). In many strains of pathogenic bacteria such as group A streptococci (*8*) and *Streptococcus pneumoniae* type 3 (74% similarity to *S. pyogenes*), UDPGlcDH provides the UDPGlcA necessary for construction of the antiphagocytic capsular polysaccharide (*9*). Mutations responsible for altered capsule formation in mutant pneumococcal capsular type 3 strains have been found to map to the gene encoding UDPGlcDH (*9*). Since proper formation of the capsular polysaccharide is essential for virulence in many pathogenic bacteria, UDPGlcDH is a logical target for the development of new antibacterial drugs.

UDPGlcDH [and its homologues UDP-*N*-acetylmannosamine dehydrogenase (UDPManNAcDH) and GDP-mannose dehydrogenase (GDPManDH)] has traditionally been classified as an NAD^+-dependent four-electron-transfer dehydrogenase along with the two other known examples: histidinol dehydrogenase and 3-hydroxy-3-methylglutaryl-coenzyme A (HMG-CoA) reductase (*1*). Although all three of these enzymes combine the enzymatic activities of both an alcohol and an aldehyde dehydrogenase in a single active site without release of an aldehyde intermediate, they lack significant sequence homology and in the case of histidinol dehydro-

[†] This research was supported in part by NSERC (graduate fellowship to R.E.C., postdoctoral fellowship to S.C.M., and operating grant to M.E.T.), NIH (Public Health Service Grant AI37320 to I.v.d.R.), and MRC (Operating Grant MT14204 to N.C.J.S.).

[‡] X-ray coordinates have been deposited in the Protein Data Bank (accession codes 1DLI and 1DLJ).

* To whom correspondence should be addressed. Phone: (604) 822-0789. Fax: (604) 822-5227. E-mail: natalie@byron.biochem.ubc.ca.

[§] Department of Chemistry, University of British Columbia.

[||] Department of Biochemistry and Molecular Biology, University of British Columbia.

[⊥] Wake Forest University Medical Center.

[1] Abbreviations: UDP, uridine-5′-diphosphoglucose; UDPGlcDH, UDP-glucose dehydrogenase; UDPGlcA, UDP-glucuronic acid; UDPManNAcDH, UDP-*N*-acetylmannosamine dehydrogenase; GDPManDH, guanosine-5′-diphosphomannose dehydrogenase; HMG-CoA, 3-hydroxy-3-methylglutaryl-coenzyme A; NAD^+, oxidized nicotinamide adenine dinucleotide; NADH, reduced nicotinamide adenine dinucleotide; NAD(H), oxidized or reduced nicotinamide adenine dinucleotide; SeMet, selenomethionine; MAD, multiwavelength anomalous dispersion; ALDH, aldehyde dehydrogenase; MurD, UDP-*N*-acetylmuramoyl-L-alanine:D-glutamate ligase; SCHAD, L-3-hydroxyacyl-CoA dehydrogenase; 6PGDH, 6-phosphogluconate dehydrogenase.

10.1021/bi000181h CCC: $19.00
Published on Web 05/18/2000

Scheme 1

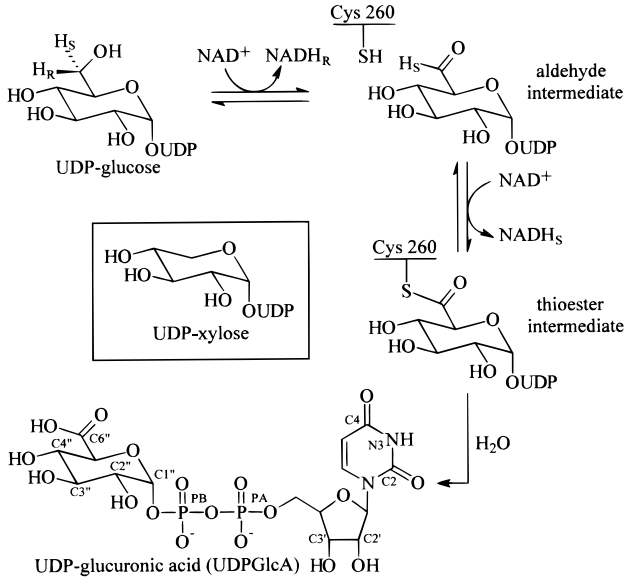

genase, a Zn^{2+}-metalloenzyme, employ distinctly different chemical mechanisms (*10*). The structure of the only other metal-independent enzyme that performs a 2-fold oxidation/reduction, HMG-CoA reductase, has been solved (*11*, *12*). This enzyme shares no structural homology with UDPGlcDH and does not utilize a nucleophilic cysteine residue since the thiol is provided by the substrate, coenzyme A.

The majority of previous studies on UDPGlcDH have focused on the bovine liver enzyme (*1*, *13*), and until recently very little was known about the bacterial enzyme (*14*). The availability of recombinant UDPGlcDH from *S. pyogenes* (*8*) prompted the first thorough investigation of the catalytic mechanism of the bacterial enzyme and has provided mounting evidence in favor of the proposed mechanism shown in Scheme 1 (*15*−*18*). The mechanism of UDPGlcDH proceeds through an initial oxidation of UDP-glucose with transfer of the C6″ *pro-R* hydride (H_R in Scheme 1) to the *si* face (B face) of NAD^+ to form NADH and the aldehyde intermediate (*1*). The order in which the C6″ hydrides are transferred to NAD^+ was originally established for the bovine enzyme (*19*) but has recently been corroborated for the *S. pyogenes* enzyme using UDP-glucose analogues (*18*). Covalent catalysis proceeds with nucleophilic attack of Cys 260 on the aldehyde to give a thiohemiacetal that is oxidized to a thioester intermediate by transfer of the remaining hydride (H_S in Scheme 1) to a second molecule of NAD^+. In the final step of the normal enzymatic reaction, the thioester intermediate is irreversibly hydrolyzed to give UDPGlcA. The involvement of a nucleophilic cysteine in covalent catalysis has been thoroughly established for both mammalian (*20*) and bacterial UDPGlcDH (*15*, *17*). The strongest evidence in support of a thioester intermediate comes from the observation that the Cys260Ser mutant incubated with either UDP-glucose or the aldehyde intermediate forms a covalently bound ester intermediate that is slowly hydrolyzed and therefore accumulates (*17*).

As described in this report, we have solved the X-ray structure of native UDPGlcDH with bound UDP-xylose and NAD^+. We have also solved the structure of Cys260Ser UDPGlcDH that was crystallized in the presence of UDP-glucose and NAD^+. Although this attempt to observe the covalent ester intermediate was unsuccessful, the structure did reveal the ternary complex of UDPGlcDH with the bound products UDPGlcA and NAD(H).

MATERIALS AND METHODS

Purification and Crystallization. UDP-glucose, UDP-xylose, NAD^+, and dithiothreitol were purchased from Sigma (St. Louis, MO). Ammonium sulfate and magnesium chloride were purchased from Fisher Scientific (Fair Lawn, NJ). For all reported procedures, Cys260Ser, selenomethionine (SeMet)-substituted and native UDPGlcDH were treated in an identical manner unless otherwise noted. SeMet was incorporated into UDPGlcDH according to the procedure of Ramakrishnan (*21*) that is available on the Internet (Ramakrishnan, V., and Graziano, V., http://snowbird.med.utah.edu/~ramak/madms/segrowth.html). UDPGlcDH was purified as previously reported (*15*) though an additional step of chromatography was necessary in order to obtain UDPGlcDH of sufficient quality for crystallization. Partially purified UDPGlcDH was applied to a column of ceramic hydroxyapatite (BioRad) in 1 mM magnesium chloride containing 10% glycerol and 2 mM dithiothreitol. The column was eluted with a linear gradient of 30−300 mM sodium phosphate (pH 6.8) in the loading buffer. To crystallize SeMet and native UDPGlcDH (differences for Cys260Ser are noted in parentheses), purified enzyme was dialyzed against 20 mM magnesium chloride, and an appropriate stock solution was added to give 5.0−5.5 mg mL^{-1} UDPGlcDH, 0.2 mM UDP-xylose (1 mM UDP-glucose), and 2 mM NAD^+ (10 mM). Crystals were grown by hanging-drop vapor diffusion from 2 to 2.1 M ammonium sulfate (1.6−1.7 M), 6−8% glycerol, and 100 mM Tris-HCl, pH 7.8. Crystals were grown at ambient temperature and generally appeared in less than 48 h and continued to grow for up to 5−6 days. Crystals had orthogonal faces with edges typically ranging from 0.05 mm to 0.3 mm in length. All crystals belonged to space group *P42(1)2* with a Matthews coefficient of 2.5, consistent with a single copy in the asymmetric unit.

Data Collection and Processing. Prior to data collection, crystals were transferred to a cryo-protectant solution of mother liquor supplemented with 25% glycerol before being flash-cooled in a stream of N_2 (100 K). Diffraction data to 3.2 Å for the multiwavelength anomalous diffraction (MAD) experiment with the SeMet UDPGlcDH crystals were collected on beamline X11 at DESY, Hamburg. Three highly redundant data sets were collected on a single crystal at wavelengths corresponding to the selenium absorption edge ($\lambda1$ = 0.9791 Å), the peak ($\lambda2$ = 0.9740 Å), and a wavelength remote from the selenium absorption edge ($\lambda3$ = 0.9200 Å). High-resolution data sets were collected for native UDPGlcDH (2.6 Å) at the same facility, and Cys260Ser UDPGlcDH (2.0 Å) at beamline X12C, Brookhaven National labs. All diffraction data were processed with DENZO/SCALEPACK (*22*), and initial phases were determined using SOLVE (*23*) which was successful in finding six of the seven selenium atoms per asymmetric unit. The SOLVE scaled structure factors and intensities were refined in SHARP (*24*) and flattened with SOLOMON (*25*).

Model Building and Structural Refinement. The SOLOMON flattened structure factors and phases produced a readily interpretable electron density map with well-defined

density for both UDP-xylose and NAD^+. XTALVIEW (*26*) was used for all model building. All 402 residues, UDP-xylose, and NAD^+ were fit in the initial round of model building and refined at full occupancy against the high-resolution Cys260Ser data set (UDP-xylose replaced with UDPGlcA) in CNS-XPLOR (*27*) utilizing rigid body minimization followed by simulated annealing and restrained *B*-factor refinement. Templates for UDP-xylose, UDPGlcA, and NAD(H) were constructed from fragments obtained from the CNS-XPLOR dictionaries or were modified versions of XPLOR (*28*) templates. Following successive cycles of model building and refinement of Cys260Ser UDPGlcDH, all 402 amino acids, UDPGlcA, NAD(H), and 390 solvent molecules were visible in the $(2F_o - F_c)$ SIGMAA (*29*) map contoured at 1σ. In addition, 3 molecules of sulfate and 3 molecules of glycerol were satisfactorily modeled into persistent $(F_o - F_c)$ density in chemically reasonable environments. These molecules were also modeled into corresponding density in the native structure though the occupancies had to be adjusted in order to maintain reasonable *B*-factors. Native UDPGlcDH was solved by molecular replacement with the final coordinates of Cys260Ser UDPGlcDH and refined in a similar manner. Both models were evaluated with the program PROCHECK (*30*) and were average or better in all statistical indicators of model quality when compared to a representative selection of refined structures at the same resolution.

The Ramachandran plot of both structures indicates a common residue, Arg 316, in the disallowed region. This residue is well ordered (Cys260Ser $B_{av} = 28$, native $B_{av} = 32$) and is tightly packed in the C-terminal domain with the guanidinium moiety forming a salt bridge with the carboxylate of Glu 349. As will be discussed, the Leu 317 to Ser 329 Ω-loop is critical for sequestering of the substrate, and the main chain conformation of Arg 316 may be relevant to this function. A second disallowed residue in the native structure, Asn 273 ($B_{av} = 33$ in both structures), is found on the surface and is stabilized by a hydrogen bond with Arg 228 of a symmetry-related molecule. Difficulties were encountered in modeling of the active site structure of the Cys260Ser mutant due to close contacts between the C6″ carboxylate of UDPGlcA, the nicotinamide ring of NAD(H), and OG of Ser 260. It was not possible to explain all the difference density in the vicinity of Ser 260 as shown in Figure 3a,b. This difference density may be the result of multiple main-chain conformations caused by unfavorable steric contacts. The more ordered nature of the crystals of Cys260Ser UDPGlcDH strongly suggests that the covalent ester form of the enzyme may have been the relevant species undergoing crystallization. However, the rate of hydrolysis in solution ($t_{1/2}$ of approximately 24−48 h at 20 °C) implies that UDPGlcA may have to exchange with UDP-glucose (and NADH with NAD^+) in the crystalline state in order to observe the ester intermediate in the X-ray structure. The apparent lack of exchange has resulted in trapping of the poorly binding product UDPGlcA ($K_I = 200\ \mu M$ compared to 2.7 μM for UDP-xylose) (*15*) and NAD(H) in an unfavorable ternary complex that is stabilized by crystal packing interactions. It is not possible to distinguish whether NAD^+ or NADH is the ligand bound to Cys260Ser UDPGlcDH, and therefore this species will be referred to as NAD(H) to reflect this uncertainty.

Analysis of Protein Structure. The primary sequence alignment included 48 sequences of UDPGlcDH, UDPManNAcDH, and GDPManDH that were retrieved from the SWISS-PROT database. The initial alignment was performed with the program CLUSTAL W (*31*) and then manipulated by hand to maximize conservation of secondary structural elements as identified by PROMOTIF (*32*). The CCP4 (*29*) programs AREAIMOL and BAVERAGE were used to determine solvent-exposed surface areas and average *B*-factors. All α-carbon superpositions were performed in the program O (*33*). Automated analysis of the dimer interface was performed by the protein−protein interaction server that is freely available on the Internet (Jones, S., and Thornton, J. M., http://www.biochem.ucl.ac.uk/bsm/PP/server). All figures of UDPGlcDH were made with BOBSCRIPT (*34*).

RESULTS

Tertiary and Quaternary Structure. UDPGlcDH consists of two discrete α/β domains, each of which contains a core β-sheet sandwiched between α-helices as shown in Figure 1. These two domains are connected by a long (48 Å) central α-helix (α9) that also serves as the core of the dimer interface. The six-stranded parallel β-sheet (β1−β4, β7, β8) that is characteristic of the dinucleotide binding Rossmann fold (*35*) serves as the core of the N-terminal NAD^+ binding domain (residues 1−196). NAD^+ is bound in a typical orientation in the cleft between strands β1 and β4, positioning the nicotinamide ring in the active site formed at the domain interface. The Rossmann fold is followed by an additional β-α-β unit (β9, α8, β10) that is antiparallel and contiguous with the central six-stranded β-sheet. However, only a single main chain hydrogen bond connects strand β8 of the six-stranded sheet and strand β9 of the antiparallel β-α-β unit, so these should probably be considered separate β-sheet structures. Inserted between β4 and α5 is a 14 residue loop (residues 80−93) that forms a small antiparallel β-sheet (β5, β6) which packs against α11 of the C-terminal domain. The last strand of the N-terminal domain (β10) leads directly into the long central α-helix (α9).

The core of C-terminal domain (residues 229−402) is a five-stranded parallel β-sheet (β11−β15) with α-helices packed on both sides. The topology of the C-terminal α/β fold (residues 310−395) is identical to the first five strands of the N-terminal dinucleotide binding fold (residues 1−115). A superposition of the α-carbons of both domains gives a rms difference of 2.0 Å over 65 atoms and is shown in Figure 2a. The predominant differences between the two regions of similar structure are two insertions (residues 41−59 and residues 80−93) in the N-terminal domain, and a single insertion (the Ω-loop) in the C-terminal domain. This interdomain pseudo-symmetry of the dinucleotide binding fold is similar to that seen in the D-specific dehydrogenases (*36*), though it has also been observed in alanine dehydrogenase (*37*), aldehyde dehydrogenase (ALDH) (*38*), and UDP-*N*-acetylmuramoyl-L-alanine:D-glutamate ligase (MurD) (*39*). In addition to the dinucleotide binding fold, the C-terminal domain also contains a stretch of three α-helices (α10−α12) that is divided by a single long stretch of extended coil (residues 242−258) that wraps around approximately half of the UDP-glucose binding pocket. This region of mixed α-helix and coil leads from the long interdomain α-helix (α9) into the five-stranded β-sheet region.

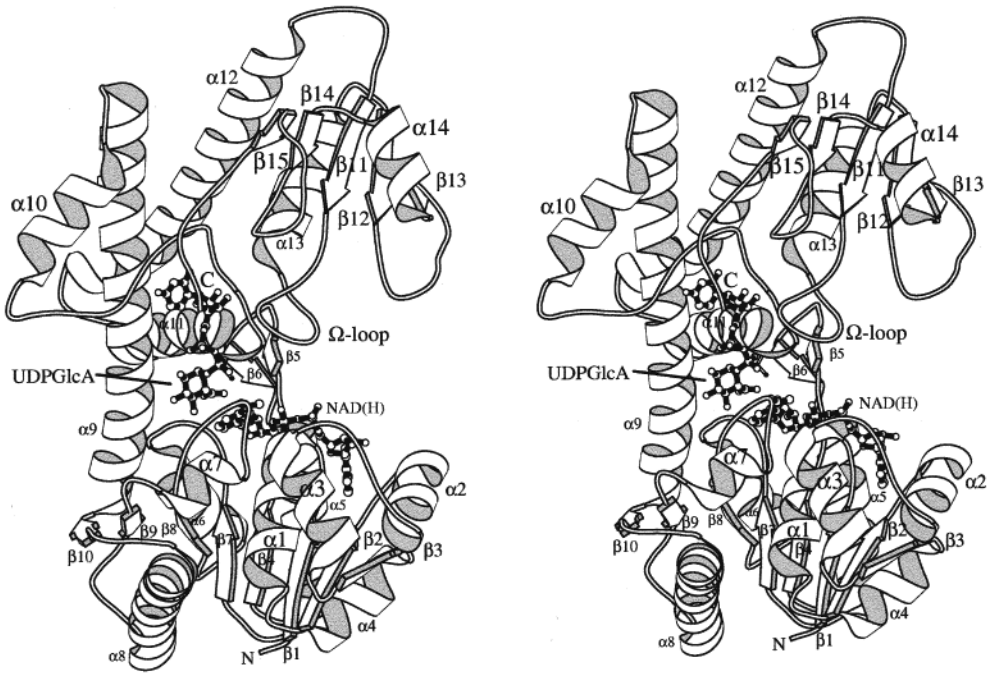

FIGURE 1: Ribbon representation of the ternary complex of the Cys260Ser UDPGlcDH/UDPGlcA/NAD(H) monomer. UDPGlcA, NAD(H), and the side chain Ser 260 (N-terminus of α11) are shown in ball-and-stick.

The C-terminal domain is primarily responsible for binding the UDP moiety of the UDP-sugar in a deep pocket approximately adjacent to the middle third of the central α-helix (α9). The UDP-sugar is orientated such that the pyranose sugar ring is positioned at the domain interface with the C6″ position of UDP-glucose (by analogy to UDPGlcA and UDP-xylose in the X-ray structures) approximately 2.5 Å from C4 (NC4) on the *si* face of the nicotinamide ring of NAD^+. Figure 3a,b illustrates the relative orientation of the UDP-sugar, NAD(H), and the catalytic nucleophile Cys 260 (Ser 260 in Figure 3b), that is found in the C-terminal domain at the N-terminus of α11. The overall structures of Cys260Ser and native UDPGlcDH are highly similar with a rms difference of 0.2 Å over all α-carbon atoms.

It is well established that bovine liver UDPGlcDH is a hexamer but due to its 'half-of-the-sites' reactivity, it may be better described as a trimer of dimers (*1*). Gel filtration studies have indicated that the *E. coli* enzyme exists as a dimer in solution (*14*). Similar experiments with the *S. pyogenes* enzyme have indicated that it may exist as a monomer in solution (*15*); however, the structure of UDPGlcDH reveals a crystallographic dimer with an interface of greater than 2600 $Å^2$ as shown in Figure 4 (*40*). The helical portion of the C-terminal domain (α10−α12) contributes the majority (52%) of the interface solvent-inaccessible surface area, followed by the central α-helix α9 (37%), and the N-terminal domain (12%). There are a total of 24 hydrogen bonds stabilizing the dimer interface, though none of the amino acids involved are strictly conserved. Aromatic residues including Phe 206, Tyr 210, Tyr 217, Tyr 224, and Tyr 272 dominate the dimer interface. Of these five residues, Tyr 210 exhibits the strongest conservation of aromatic character, and it is interesting to note that this residue interacts with itself through crystallographic symmetry. Tyr 217 is noteworthy as it exhibits strong conservation of aromatic or hydrophobic character in all bacteria, though higher order species have a serine at this position.

Structural Similarity to Other Dehydrogenases. The program DALI (*41*) was used to search for homologous proteins, and as expected, many dehydrogenases and related proteins containing dinucleotide binding domains were identified as being structurally similar. The proteins with the greatest overall structural homology to UDPGlcDH are short-chain L-3-hydroxyacyl-CoA dehydrogenase (SCHAD) (*42*) and 6-phosphogluconate dehydrogenase (6PGDH) (*43*). Structural alignment of residues 1−290 of UDPGlcDH with each of these two proteins gives a rms difference of 1.9 Å in both cases over 163 and 168 α-carbons respectively as shown for 6PGDH in Figure 2b. All the major secondary structural elements of the N-terminal domain as well as significant portions of the central α-helix (α9) and the C-terminal α-helical region (α10−α12) are common to UDPGlcDH, SCHAD, and 6PGDH. Beyond residue 290 of UDPGlcDH, there is no structural homology with either SCHAD or 6PGDH as both of these proteins have a primarily α-helical domain whereas UDPGlcDH has the C-terminal dinucleotide binding fold. While the reactions catalyzed by both SCHAD and 6PGDH are similar (*β*-oxidation and *β*-oxidation/decarboxylation respectively), they are fundamentally different from UDPGlcDH (2-fold oxidation followed by hydrolysis) which leads one to speculate on the foundation for this structural relationship. The basis for this relationship may be the conservation of the NAD^+ binding domain as well as active site architecture and specific catalytic residues that are common to both enzymes. Inspection of the active site of 6PGDH superimposed with UDPGlcDH revealed a remarkable conservation of identity and conformation for two active site residues: Lys 204 and Asn 208 (Lys 183 and Asn 187 in sheep liver 6PGDH). These residues have been implicated in the enzymatic mechanism of 6PDGH (*43*, *44*), and their possible roles in the mechanism of UDPGlcDH will be discussed below.

Roles of Conserved Residues. Alignment of 48 sequences including UDPGlcDH, UDPManNAcDH, and GDPManDH

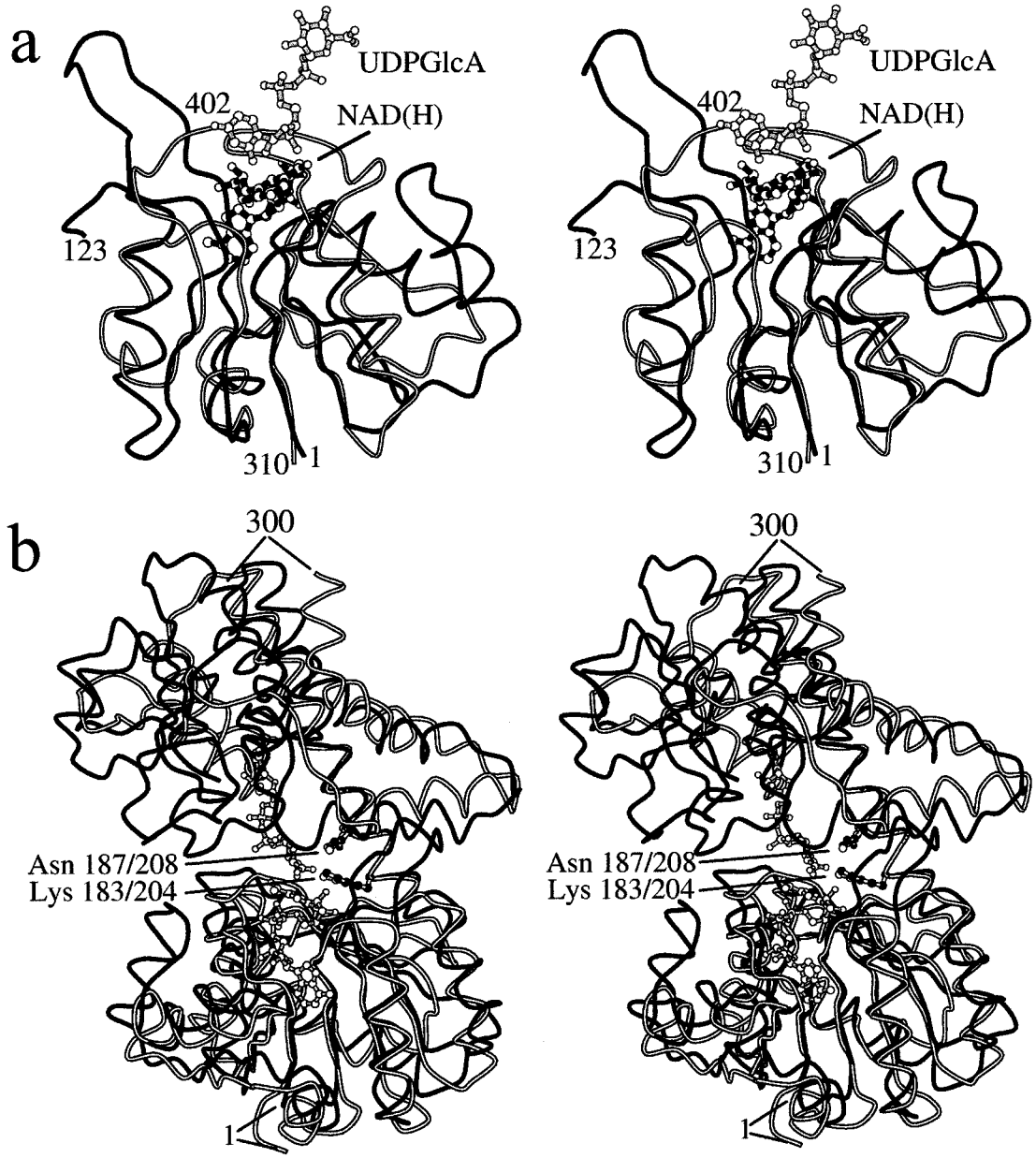

FIGURE 2: (a) Superposition of the α-carbons of residues 1−123 (black coil) and NAD(H) (black bonds) with residues 310−402 (white coil) and UDPGlcA (gray bonds) of Cys260Ser UDPGlcDH. The orientation of UDPGlcA bound to the C-terminal dinucleotide binding fold is distinctly different from the normal mode of NAD^+ binding. (b) Superposition of the α-carbons of Cys260Ser UDPGlcDH (black coil) and residues 1−300 of 6PGDH (white coil). In addition to UDPGlcA and NAD(H) bound to Cys260Ser UDPGlcDH, the side chains of the conserved residues Lys 204 and Asn 208 of UDPGlcDH (gray bonds with white atoms) and Lys 183 and Asn 187 of 6PGDH (white bonds with black atoms) are indicated.

revealed a total of 22 residues that were strictly conserved in 47 or more sequences. A representative selection of sequences from this alignment is shown in Figure 5. All secondary structural elements appear to be conserved across the 48 sequences, with the greatest sequence diversity occurring near the C-terminus, as exemplified by the approximately 50 additional residues in the mammalian UDPGlcDH. Of the 22 conserved residues, 6 are primarily involved in binding NAD^+, 2 are involved in binding UDP-glucose, and a total of 10 residues either are directly involved in catalysis or are critical for the proper positioning of the catalytic groups. These residues will be discussed below in the context of substrate binding and the catalytic mechanism.

The four remaining strictly conserved residues (Ser 161, Glu 201, Asn 219, and Asn 287) are all remote from both the active site and the substrate binding pockets so are likely important for maintaining structural integrity or are necessary for productive folding. Interestingly, the relatively conservative mutation Glu201Asp results in an unencapsulated phenotype in mutant strains of *S. pneumonia* (*9*). The carboxylate of Glu 201 forms buried hydrogen bonds with the main chain amide nitrogens of three residues (Gly 122, Phe 123, and Ile 124) located at the dimer interface. Disruption of these critical hydrogen bonds would likely interfere with proper formation of the dimeric species and may additionally alter the position of Thr 118, a critical active site residue that is close in primary sequence.

Substrate Binding. The fold of the C-terminal UDP-glucose binding domain is homologous to the ubiquitous dinucleotide binding fold, so it is extraordinary that the

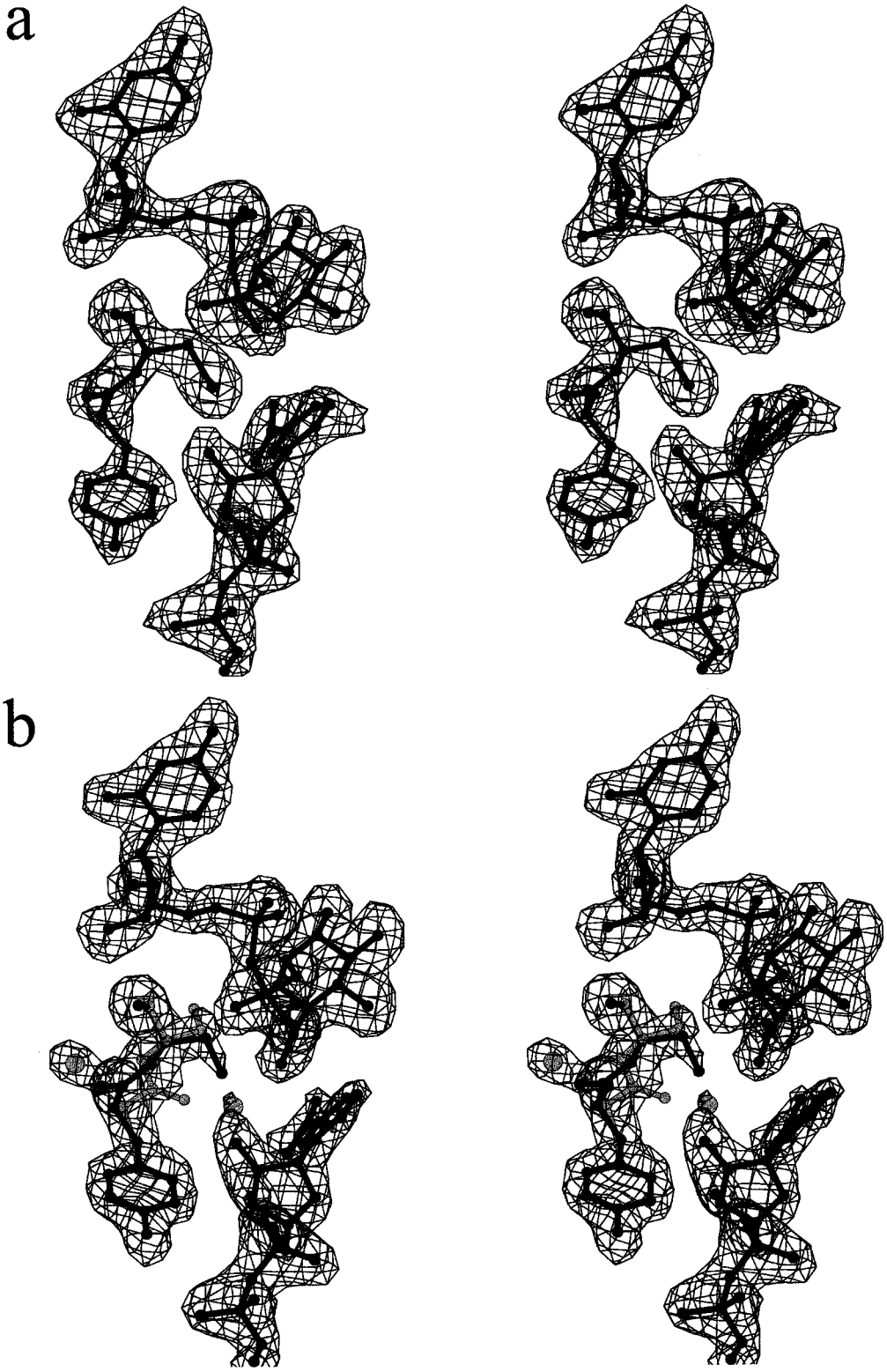

FIGURE 3: Representative electron density for NAD(H), the UDP-sugar, and residues 259−260. The adenosine portion of NAD(H) is not shown. For both native and Cys260Ser UDPGlcDH, a ($F_o - F_c$) map was calculated with the final model coordinates lacking NAD(H), the UDP-sugar, and residues 259−260. The map was calculated with all data to 2.3 and 1.8 Å, respectively, and was contoured at 3σ. (a) Native UDPGlcDH shows well-defined density for UDP-xylose, NAD^+, and both Tyr 259 and Cys 260. (b) Cys260Ser UDPGlcDH clearly shows the bound UDPGlcA and NAD(H), but Tyr 259 and Ser 260 have additional density that is not adequately explained by the final model (black ball-and-stick). A proposed alternate conformation of the Tyr 259−Ser 260 peptide bond and the OG of Ser 260 is shown in gray with two associated water molecules.

orientation of substrate binding has no apparent relation to the normal orientation of NAD^+ binding as clearly shown in Figure 2a. In the X-ray structure of MurD (*39*), the substrate (a UDP-sugar) is bound to the N-terminal Rossmann fold in an orientation similar to NAD^+. In UDPGlcDH, the orientation of the bound UDP-sugar relative to NAD(H) is reminiscent of substrate binding in the abortive complex of UDP-galactose 4-epimerase with UDP-glucose and NADH

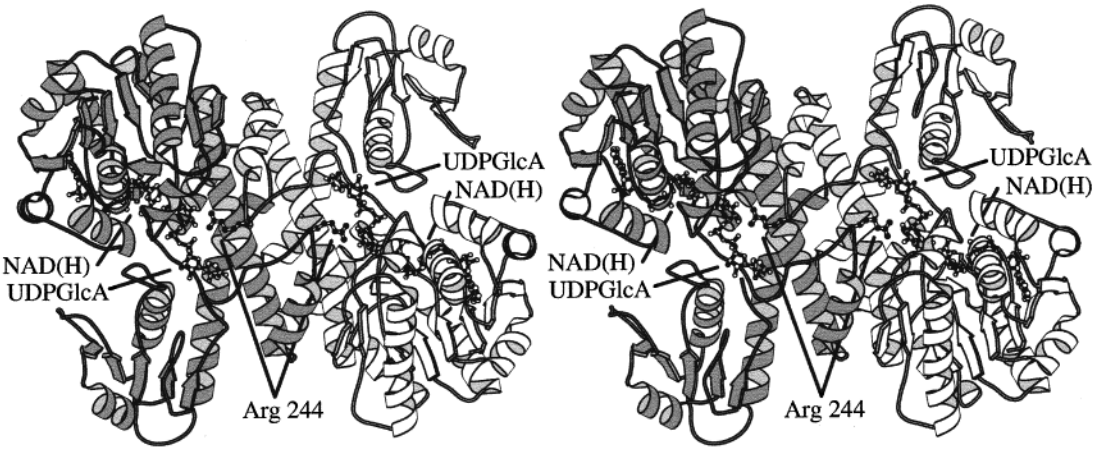

FIGURE 4: Crystallographic dimer of Cys260Ser UDPGlcDH. Indicated in the figure is the side chain of Arg 244 that forms hydrogen bonds with the substrate of the dimer partner.

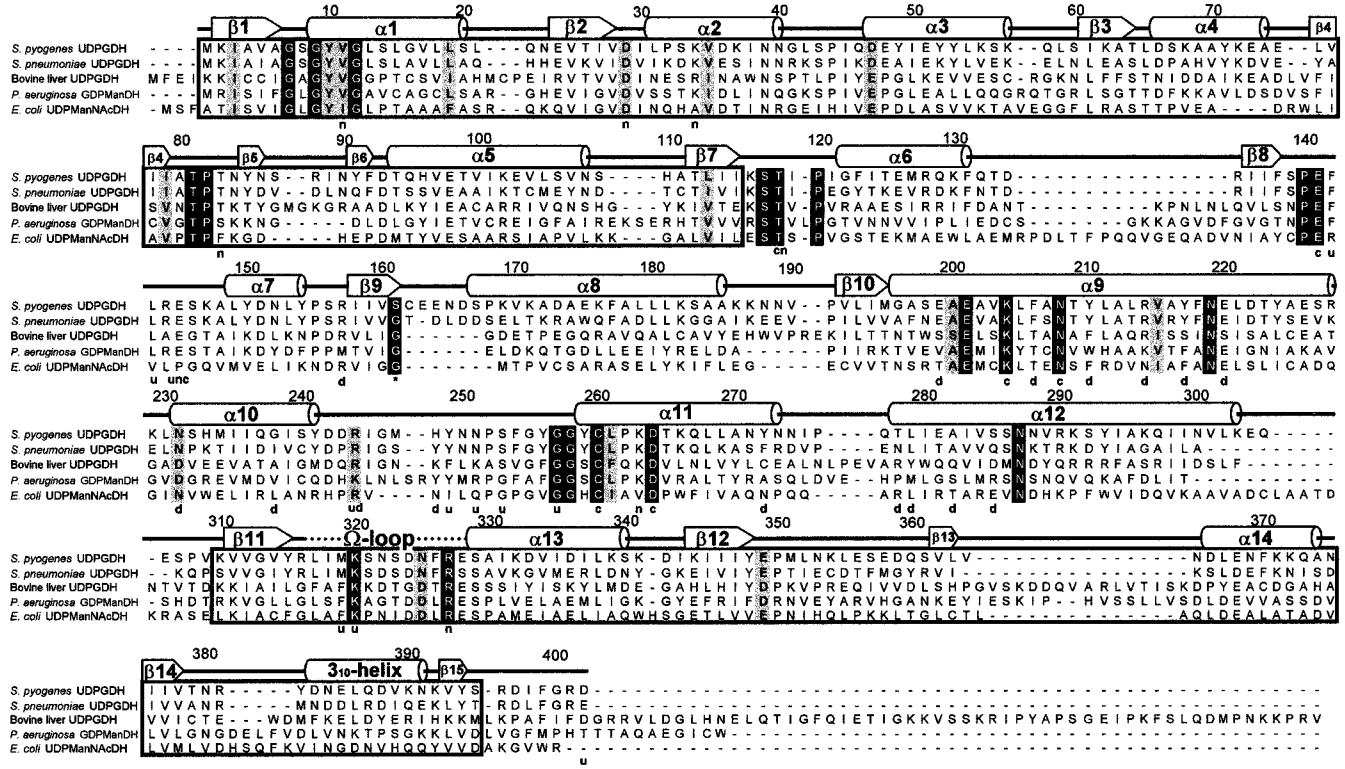

FIGURE 5: Representative primary sequence alignment of 48 sequences that include UDPGlcDH, UDPManNacDH, and GDPManDH. Secondary structural elements are shown schematically with cylinders representing α-helices and arrows representing *β*-strands. The two boxed areas correspond to the regions of similar fold superimposed in Figure 2a. Positions in the sequence that are highlighted with white text on a black background are strictly conserved in at least 47 of the 48 aligned sequences while positions highlighted in gray exhibit strong conservation. The one-letter code directly below the aligned sequences indicates a hydrogen bond to either NAD(H) (n), the UDP-sugar (u), or the dimer partner (d). Putative catalytic residues mentioned in the text are also indicated (c). Residue 161 (indicated by *), meets the above criteria for strict conservation, but *S. pyogenes* is the only divergent sequence.

(*45*). Despite the lack of structural homology in the UDP-sugar binding regions of these two enzymes, there are several apparent similarities in the protein−substrate interactions. Both enzymes make similar main chain hydrogen bonding interactions with the uridine moiety and utilize a carboxylate group to form a hydrogen bond with the ribose C2′ hydroxyl. The UDP-glucose binding pocket of UDPGlcDH, which is schematically represented in Figure 6, can be divided into two regions: the UMP binding pocket which is composed solely of residues contributed from the C-terminal domain, and the glucose 1-phosphate binding pocket consisting primarily of residues from the N-terminal domain. The UMP binding pocket is lined with a stretch of coil (Tyr 249−Gly 257) that makes three main chain hydrogen bonds, two side chain hydrogen bonds, and a *π*-edge stacking interaction of Tyr 249 with the UMP moiety. The residues involved in these interactions include the strictly conserved Gly 257 that forms a hydrogen bond with the ribose C3′ hydroxyl of UMP. There is one strictly conserved charged residue, Lys 320, that forms a salt bridge with the pyrophosphate moiety and is probably critical for sequestering of the substrate from the bulk solvent as will be discussed. Although the glucose 1-phosphate

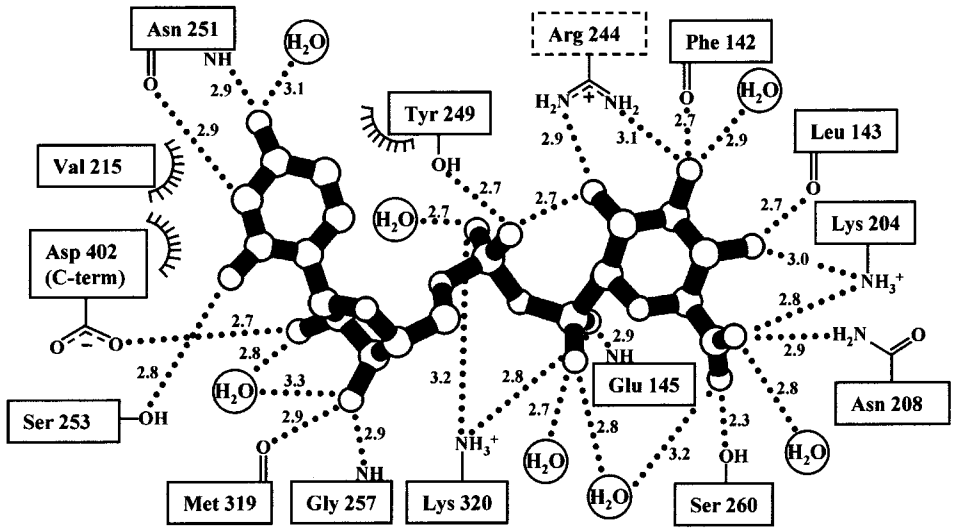

FIGURE 6: Schematic representation of interactions and hydrogen bond distances (Å) between UDPGlcDH and bound UDPGlcA. The conformations of UDPGlcA bound to Cys260Ser UDPGlcDH and UDP-xylose bound to native UDPGlcDH are very similar (rms difference = 0.2 Å) and so are their interactions with the enzyme. Arg 244 (dashed box) is contributed by the symmetry-related dimer partner.

Table 1: Data Collection and Phasing Statistics

	SeMet UDPGlcDH				
	$\lambda 1$	$\lambda 2$	$\lambda 3$	native	Cys260Ser
wavelength (Å)	0.9791	0.9740	0.9200	0.9057	0.9790
resolution range (Å)	19.8−3.20	20.0−3.20	20.0−3.20	24.3−2.30	27.8−1.80
mosaicity (deg)	0.3	0.3	0.3	1.2	0.8
completeness (%)[a]	100 (100)	100 (100)	100 (100)	95.1 (76.2)	87.3 (42.4)
observations	78626	62644	64705	119755	176474
unique observations	8176	8056	8118	20014	38511
R_{merge} (%)[a,b]	12.4 (29.8)	12.6 (30.5)	12.9 (33.4)	8.2 (37.7)	4.5 (51.0)
I/σ[a]	19.1 (7.7)	18.2 (7.7)	18.5 (7.4)	18.5 (2.7)	28.8 (1.7)
phasing statistics					
dispersive phasing power[c] (centrics/acentrics)	2.14/3.18	2.87/3.68	0/0		
anomalous phasing power[c]	1.43	1.66	1.34		
R_{cullis} dispersive[d] (centrics/acentrics)	0.51/0.48	0.53/0.52	0/0		
R_{cullis} anomalous[d]	0.89	0.83	0.91		

[a] Values in parentheses are for the outermost shell which is 3.27−3.20 Å for SeMet data, 2.34−2.30 Å for native, and 1.83−1.80 Å for Cys260Ser. The highest resolution shell with at least 50% of the data with I/σ greater than 3 is 2.08−2.03 Å for Cys260Ser and 2.73−2.66 Å for native. [b] $R_{merge} = \sum|I - \langle I\rangle|/\sum I$. [c] Phasing power = (rms F_h)/(rms E), where F_h is the heavy-atom structure amplitude and E is the residual lack of closure error. [d] $R_{cullis} = \sum|E|/\sum|\Delta F|$.

binding pocket is found at the dimer interface, binding interactions are limited to a small region (Phe 142−Glu 145) between β7 and α7 of the N-terminal domain that forms three main chain hydrogen bonds to the glucose 1-phosphate moiety. The glucose 1-phosphate binding pocket contains one additional residue contributed from the dimer partner. Arg 244 extends into the adjacent active site, forming hydrogen bonds with the pyranose C2″ and C3″ hydroxyls, and may assist in proper orientation of the substrate for oxidation (see Figures 4 and 6). Arg 244 reveals a clear mechanism for communication between active sites of the dimer pair, and UDPGlcDH from *S. pyogenes* has been noted to exhibit weak allosteric effects (Hill coefficient less than 1.5) (*16*). This is in marked contrast to the mammalian enzyme that exhibits very strong allosteric effects resulting in the observed 'half-of-the-sites' reactivity (*1*). Interestingly, sequence alignments show that Arg 244 may be a determinant of substrate specificity as it appears to be conserved through all UDPGlcDH and UDPManNAcDH, but is replaced by a lysine residue in GDPManDH (see Figure 5).

NAD(H) is bound to the N-terminal domain of UDPGlcDH in a typical orientation with the nicotinamide ring in a syn conformation. All hydrogen bonds between UDPGlcDH and NAD(H) are listed in Table 3. The *si* face of the nicotinamide ring is facing the UDP-sugar, and the *re* face is packed against a hydrophobic patch composed of Val 11, Leu 143, and Glu 141 (CB and CG). Six of the strictly conserved residues of UDPGlcDH are primarily involved in binding NAD^+: the three glycines of the GxGxxG 'fingerprint' of the Rossmann fold, the Thr 81/Pro 82 pair that packs against the adenine ring of NAD^+, and Arg 327 that forms

Table 2: Refinement and Model Statistics

	native	Cys260Ser
resolution range (Å)	24−2.3	28−1.8
observations	20008	38487
R_{factor}[a] (%)	18.6	17.9
R_{free}[b] (test set, %)	25.9	21.3
model statistics		
rmsd bonds (Å)	0.011	0.011
rmsd angles (deg)	1.6	1.5
fully allowed ϕ,ψ (%)	89.0	89.0
disallowed ϕ,ψ (%)	0.5	0.3

[a] $R_{factor} = \sum|F_{obs} - F_{calc}|/|F_{obs}|$. [b] R_{free} was calculated on 10% of the reflections that were randomly omitted from the refinement.

Table 3: NAD(H)−UDPGlcDH Hydrogen Bond Distances

residue	NAD(H)[a]	distance[b] (Å)
Val 11 N	NO2	3.1 (3.1)
Asp 29 OD1	AO2*	2.8 (2.6)
Asp 29 OD2	AO3*	2.7 (2.7)
Lys 34 NZ	AO3*	3.0 (3.0)
Thr 83 OG1	NO3*	2.5 (2.5)
Thr 118 N	NO3*	3.2 (3.0)
Glu 145 OE2	NN7	3.1 (3.2)
Lys 263 NZ	NO2*	2.9 (2.7)
Arg 327 NH1	AO1	3.1 (3.4)
Arg 327 NH2	NO1	2.9 (3.2)

[a] Atom names for NAD(H) follow the PDB convention. [b] Distances are given for Cys260Ser/NAD(H) followed by native/NAD^+ in parentheses.

a salt bridge with the pyrophosphate. Asp 29 is a critical residue of the dinucleotide binding 'fingerprint' and exhibits strict conservation of either aspartate or glutamate that can hydrogen bond to both hydroxyls (AO2* and AO3*) of the adenine ribose.

Sequestering of Reaction Intermediates. A defining characteristic of the UDPGlcDH family of enzymes is the inability to detect the transient formation of any intermediates at the oxidation level of an aldehyde (*1*). This negative result had contributed to the previous proposal that the aldehyde intermediate is covalently bound to the enzyme as an imine (*1*). An inspection of the structure of UDPGlcDH reveals a deeply buried active site that only exposes 5 $Å^2$ of the UDP-sugar to the bulk solvent. This is in contrast to NAD^+ which must freely exchange during the catalytic mechanism and has a solvent-accessible area of approximately 54 $Å^2$. To permit reversible binding of a UDP-sugar, UDPGlcDH would require either a significant interdomain movement and/or a repositioning of a loop region that covers the substrate. This is consistent with the observation that extensive screening of crystallization conditions in the absence of UDP-sugars and NAD^+ failed to produce crystals of free UDPGlcDH, suggesting that there is a conformational ordering upon substrate binding that is conducive to crystallization. The protein surface that buries the UDP-sugar is composed of four separate regions that together shield 156 $Å^2$ of UDP-GlcA (Cys260Ser UDPGlcDH) from the bulk solvent. These regions are composed of the Ω-loop (53 $Å^2$), the C-terminus (33 $Å^2$), the side chain of Arg 244 (8 $Å^2$), and the Arg 144−Lys 147 β-turn (62 $Å^2$). Of these four regions, the Ω-loop is the best candidate for a mobile 'gate' that opens and closes to allow reversible substrate binding. The Ω-loop is present in all aligned sequences of UDPGlcDH (see Figure 5) and contains two strictly conserved residues, Lys 320 and Arg 327, which form salt bridges with the pyrophosphate moieties of the UDP-sugar and NAD(H), respectively. The salt bridges formed by Lys 320 and Arg 327 are the predominant interactions locking the 'gate' in the 'closed' conformation, and in the absence of substrate, the Ω-loop may adapt an alternative 'open' conformation. The C-terminus (Asp 402) makes several contacts with both the UDP moiety and the Ω-loop, and movement of either of these groups would also require a reorientation of the C-terminus, implying that it may be a second component of the active site 'gate'. As suggested earlier, to explain the apparent lack of substrate exchange in the crystalline state, it is believed that the 'gate' is forced to maintain its 'closed' conformation due to crystal packing interactions. Since there are no direct crystal contacts with the Ω-loop, opening of the 'gate' may be associated with a significant global conformational change that is unfeasible within the crystalline lattice.

Active Site Residues of UDPGlcDH. As illustrated in Figure 7a,b, the active site of UDPGlcDH contains the side chains of six conserved residues that are contributed from the N- and C-terminal domains as well as from the central α-helix (α9). From the N-terminal domain, Thr 118 of the conserved loop between β7 and α6 forms a hydrogen bond to an ordered and conserved active site water molecule (Cys260Ser $B = 21$, native $B = 23$) that may be critical for the catalytic mechanism. Flanking Thr 118 in the primary sequence are the strictly conserved Ser 117 and Pro 120 that are probably essential for proper orientation of the catalytic Thr 118. A strictly conserved pair of residues in the N-terminal domain, Pro 140/Glu 141 (between β8 and α7), position the carbonyl oxygen of Glu 141 such that a hydrogen bond is formed to NZ of the key catalytic residue Lys 204. An additional active site residue and an apparent determinant of substrate specificity, Glu 145 exhibits very strong conservation across all sequences of UDPGlcDH and GDPManDH but is replaced by a proline in UDPManNAcDH. Glu 145 forms a hydrogen bond to a conserved water molecule (Cys260Ser $B = 36$, native $B = 41$) that is in turn coordinated to a phosphate (PB) oxygen in both structures and a C6″ carboxylate oxygen (O6″2) in Cys260Ser UDPGlcDH.

The central α-helix (α9) contributes two strictly conserved active site residues, Lys 204 and Asn 208, which coordinate a carboxylate oxygen (O6″1) of UDPGlcA in Cys260Ser and a similarly positioned active site water ($B = 39$) in the native structure. Other than the catalytic nucleophile Cys 260, Asp 264 is the only other conserved residue in the C-terminal domain that extends into the active site and probably has a direct role in the enzyme mechanism. Both Cys 260 and Asp 264 are situated in the strictly conserved active site signature sequence, GGxCxxxD (see Figure 5), that is characteristic of UDPGlcDH. The strictly conserved glycine pair preceding Cys 260 suggests that main chain conformations inaccessible to non-glycine residues are required for proper orientation of the catalytic nucleophile during catalysis. This is well precedented within the ALDH extended family where a strictly conserved glycine residue precedes the catalytic cysteine and is necessary to allow the polypeptide chain to 'twist back on itself' (*46*).

DISCUSSION

In the first step of the catalytic mechanism, UDPGlcDH oxidizes the primary C6″ hydroxyl of UDP-glucose with transfer of the *pro-R* hydride to C4 (NC4) on the *si* face of the nicotinamide ring of NAD^+ (see Scheme 1). It is well precedented that enzymatic alcohol oxidation requires a general base: a role performed by a tyrosine hydroxyl in the short-chain dehydrogenases/reductases (*47*) and a histidine imidazole in lactate dehydrogenase (*48*). HMG-CoA reductase has been proposed to utilize a lysine general base to deprotonate the alcohol (in the direction of oxidation) as well as to stabilize the oxyanion of the hemiacetal intermediate (*12*). A conserved arginine residue in the active site of HMG-CoA reductase may serve to depress the lysine pK_a through electrostatic interactions so it can serve as a base.

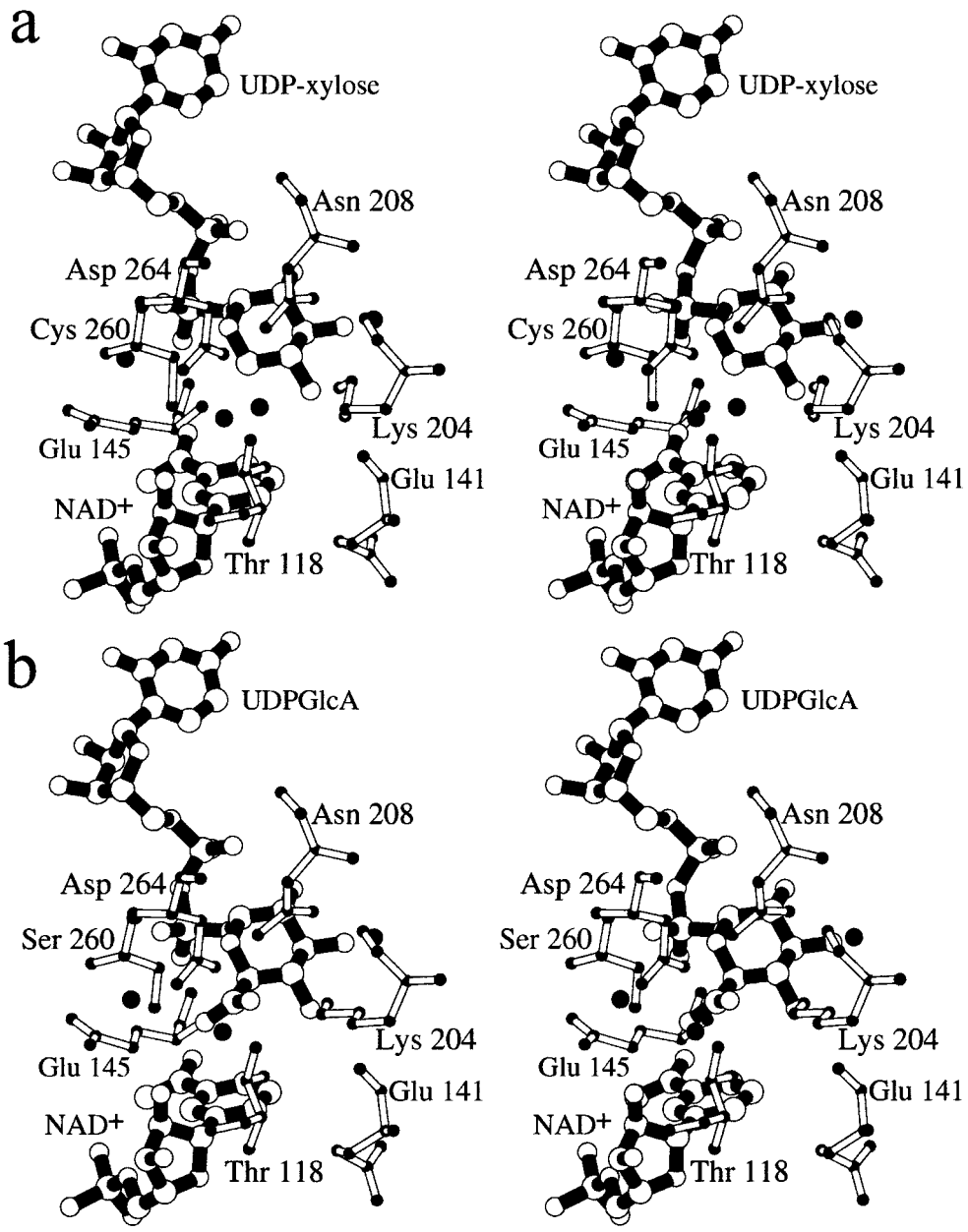

FIGURE 7: Close-up views of the active site of UDPGlcDH with putative catalytic residues. (a) The active site of native UDPGlcDH with bound UDP-xylose and NAD^+ truncated at the pyrophosphate bond. (b) The active site of Cys260Ser UDPGlcDH with bound UDPGlcA and NAD(H). Notice that the C6″ carboxylate of UDPGlcA occupies a position similar to a water molecule in the native structure.

In UDPGlcDH, the known stereochemistry of the first hydride transfer and the observed orientation of the UDP-sugar and NAD^+ in the X-ray structure fix the relative position of the catalytic base that must deprotonate the substrate alcohol. The C6″ hydroxyl of the substrate, UDP-glucose, probably occupies a position similar to the carboxylic acid oxygen (O6″1) of UDPGlcA in the Cys260Ser structure and the similarly positioned water molecule in the native structure (see Figure 7a,b). Lys 204 (NZ) is the closest residue (2.8 Å) to this position (2.9 Å in native/UDP-xylose), and based on the precedence of HMG-CoA reductase, it is tempting to propose that Lys 204 is the general base responsible for deprotonation of the substrate alcohol as shown in Figure 8a. As mentioned above, Lys 204 is structurally analogous to Lys 183 of 6PGDH, and therefore may perform a similar function in the catalytic mechanism. Recent evidence has provided support for Lys 183 of 6PGDH acting as the general base for deprotonation of the substrate alcohol (*44*). It was proposed that the hydrophobic nature of the 6PGDH active site could perturb the pK_a of Lys 183 by approximately 2.5 pH units to a pK_a of 8. In the ternary complex of UDPGlcDH, Lys 204 is inaccessible to bulk solvent, but there are no positively charged residues or extensive hydrophobic regions in the immediate vicinity of Lys 204 (NZ) that should significantly lower the pK_a. However, UDPGlcDH has a relatively basic pH−rate optimum (pH 9), so invoking a substantially depressed pK_a for Lys 204 may not be necessary.

An alternative candidate for the role of the general base is the conserved water molecule that is activated due to its hydrogen bond (2.6 Å in both structures) to the Asp 264 carboxylate as shown in Figure 8b. This tetrahedrally coordinated water molecule also forms a hydrogen bond (2.8 Å) with the carboxylate oxygen (O6″1) of UDPGlcA in

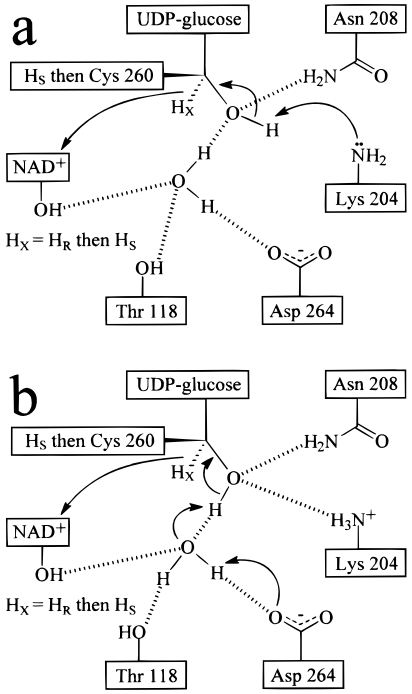

FIGURE 8: Two possible mechanisms for the 2-fold oxidation of UDP-glucose ($H_X = H_R$) to the aldehyde intermediate and the thiohemiacetal intermediate ($H_X = H_S$) to the thioester intermediate. (a) The general acid/base catalyst is assumed to be Lys 204. The base is responsible for deprotonating the alcohol substrate during the first oxidation and contributing to stabilization of the tetrahedral intermediate during the second oxidation. (b) The general acid/base catalyst is assumed to be the water molecule that is rendered basic due to its coordination with Asp 264. The hydrogen bonding environment of Thr 118 does not preclude this residue acting as either a donor or an acceptor with the putative catalytic water molecule.

Cys260Ser (2.4 Å to the similarly positioned water in the native/UDP-xylose structure). Additional hydrogen bonds with the strictly conserved residue Thr 118 and a ribose hydroxyl of NAD^+ (NO2*) are likely critical for proper positioning of this putative catalytic water. In this proposed mechanism, Lys 204 NZ and Asn 208 ND1 could participate in the first oxidation through electrostatic stabilization of the alkoxide form of the substrate alcohol. It is relevant to note that the only known divergent sequence at position 204 (*Shigella sonnei*, SWISS-PROT accession number Q55042, not shown in Figure 5) is a glutamine residue that could provide electrostatic stabilization but not act as an acid/base catalyst.

A strictly conserved mechanistic feature of all aldehyde oxidations that utilize covalent catalysis is the requirement for a nucleophilic thiol. To increase the nucleophilic character of the thiol, enzymes may utilize an adjacent base such as histidine as proposed for both glyceraldehyde-3-phosphate dehydrogenase (*49*) and HMG-CoA reductase (*12*). In order for the thiol of Cys 260 to attack the *si* face of the aldehyde intermediate and generate the appropriate tetrahedral geometry for the second hydride transfer (see Figure 8a,b), a rotation from gauche(+) to gauche(−) may be necessary. This rotation could be accompanied by other conformational changes that could orient an appropriate base, such as the water activated by Glu 145, to deprotonate the thiol. It is interesting to note that the UDPGlcDH pH−rate optimum of pH 9 is consistent with the normal pK_a of a cysteine thiol and suggests that an assisting base may not be necessary.

The oxidation of UDP-glucose to the aldehyde intermediate generates a proton donor (either Lys 204 or the water molecule activated by Asp 264) that would be strategically positioned to participate as a general acid catalyst during the subsequent attack of the cysteine thiol on the aldehyde intermediate (see Figure 8a,b). The oxyanion of the tetrahedral thiohemiacetal could be stabilized by Asn 208 and the catalytic moiety (Lys 204 or the water molecule activated by Asp 264) not involved in general acid catalysis. Collapse of the tetrahedral intermediate with hydride transfer to NAD^+ and proton transfer back to the catalytic base would yield the covalently bound thioester. The proposed role for Asn 208 is similar to the conserved active site asparagine in the ALDH extended family that has been proposed to coordinate the carbonyl oxygen of the substrate (*46*). In the final step of the reaction, nucleophilic attack by a basic water molecule on the thioester would once again yield a tetrahedral intermediate. To generate a tetrahedral intermediate with geometry analogous to the thiohemiacetal, the hydrolytic water must add to the face of the thioester that is blocked by NADH. This argument leads to two possibilities: either NADH dissociates prior to the final hydrolysis or the tetrahedral intermediate formed during hydrolysis is not strictly analogous to the thiohemiacetal and there is a conformational change that moves the covalent thioester away from NADH. In support of the former option, the strictly conserved Glu 141 is located beneath the nicotinamide ring (see Figure 7a,b), and in the absence of NADH could extend into the active site and deliver an activated water molecule to the thioester. It is not known if NADH dissociates from UDPGlcDH before hydrolysis of the thioester intermediate.

The structure of UDPGlcDH reported here represents the first ever look at how the catalytic machinery of a single active site can perform the 2-fold oxidation of a primary alcohol to the free acid product. The overall fold of UDPGlcDH has been described for the first time and consists of a classical NAD^+ binding domain that exhibits remarkable structural homology with 6-phosphogluconate dehydrogenase. The C-terminal UDP-sugar binding domain also contains a dinucleotide binding fold; however, this structure is suprisingly not exploited for binding of the substrate in a typical orientation. The two domains are connected by a long central α-helix that serves as the core of the dimer interface. A structure-based sequence alignment has confirmed the catalytic importance of several active site residues and has allowed for the first detailed proposal of the mechanism of UDPGlcDH. The structural evidence argues in favor of general acid/base, electrostatic, and covalent catalysis participating in the three discrete yet mechanistically similar steps of the overall reaction. Two candidates (Lys 204 or the water molecule activated by Asp 264) for the critical base in the catalytic mechanism have been proposed, and further studies will be required in order to distinguish these two possibilities. This insight into the structure and mechanism of UDPGlcDH should greatly facilitate efforts toward structure-based inhibitors and potential antibiotics to specifically combat pathogens such as *S. pneumoniae* and group A streptococci.

ACKNOWLEDGMENT

We thank Shouming He for performing electrospray mass spectrometry and Mark Paetzel for assistance in synchrotron data collection. We are grateful to the Department of Energy and the NSL at Brookhaven as well as the EMBL(DESY) at Hamburg for access to their respective synchrotron radiation sources. Additional thanks go to R. Sweet and W. Rypniewski for assistance in data collection.

REFERENCES

1. Feingold, D. S., and Franzen, J. S. (1981) *Trends Biochem. Sci. 6*, 103−105.
2. Strominger, J. L., Kalckar, H. M., Axelrod, J., and Maxwell, E. S. (1954) *J. Am. Chem. Soc. 76*, 6411−6412.
3. Spicer, A. P., Kaback, L. A., Smith, T. J., and Seldin M. F. (1998) *J. Biol. Chem. 273*, 25117−25124.
4. Dutton, G. J. (1980) in *Glucuronidation of drugs and other compounds*, CRC Press, Boca Raton, FL.
5. Rodén, L. (1980) in *The Biochemistry of Glycoproteins and Proteoglycans* (Lennarz, W. J., Ed.) pp 267−371, Plenum Publishing Co., New York.
6. Binari, R. C., Staveley, B. E., Johnson, W. A., Godavarti, R., Sasisekharan, R., and Manoukian, A. S. (1997) *Development 124*, 2623−2632.
7. Dalessandro, G., and Northcote, D. H. (1977) *Biochem. J. 162*, 267−279.
8. Dougherty, B. A., and van de Rijn, I. (1993) *J. Biol. Chem. 268*, 7118−7124.
9. Arrecubieta, C., Lopez, R., and Garcia, E. (1994) *J. Bacteriol. 176*, 6375−6383.
10. Grubmeyer, C., and Teng, H. (1999) *Biochemistry 38*, 7355−7362.
11. Lawrence, C. M., Rodwell, V. W., and Stauffacher C. V. (1995) *Science 268*, 1758−1762.
12. Tabernero, L., Bochar, D. A., Rodwell, V. W., and Stauffacher C. V. (1999) *Proc. Natl. Acad. Sci. U.S.A. 96*, 7167−7171.
13. Hempel J., Perozich, J., Romovacek, H., Hinich, A., Kuo, I., and Feingold, D. S. (1994) *Protein Sci. 3*, 1074−1080.
14. Schiller, J. G., Bowser, A. M., and Feingold, D. S. (1973) *Biochim. Biophys. Acta 293*, 1−10.
15. Campbell, R. E., Sala, R. F, van de Rijn, I., and Tanner, M. E. (1997) *J. Biol. Chem. 272*, 3416−3422.
16. Campbell, R. E., and Tanner, M. E. (1997) *Angew. Chem., Int. Ed. Engl. 13/14*, 1520−1522.
17. Ge, X., Campbell, R. E., van de Rijn, I., and Tanner, M. E. (1998) *J. Am. Chem. Soc. 120*, 6613−6614.
18. Campbell, R. E., and Tanner, M. E. (1999) *J. Org. Chem. 64*, 9487−9492.
19. Ridley, W. P., and Kirkwood, S. (1973) *Biochem. Biophys. Res. Commun. 54*, 955−960.
20. Ridley, W. P., Houchins, J. P., and Kirkwood, S. (1975) *J. Biol. Chem. 250*, 8761−8767.
21. Ramakrishnan, V., Finch, J. T., Graziano, V., Lee, P. L., and Sweet, R. M. (1993) *Nature 362*, 219−223.
22. Otwinowski, Z., and Minor, W. (1997) *Methods Enzymol. 276*, 307−325.
23. Terwilliger, T. C., and Berendzen, J. (1997) *Acta Crystallogr. D53*, 571−579.
24. De La Fortelle, E., and Bricogne, G. (1997) *Methods Enzymol. 276*, 472−494.
25. Abrahams, J. P., and Leslie, A. G. W. (1996) *Acta Crystallogr. D52*, 30−42.
26. McRee, D. E. (1992) *J. Mol. Graphics 10*, 44−46.
27. Brünger, A. T., Adams, P. D., Clore, G. M., Gros, P., Grosse-Kunstleve, R. W., Jiang, J.-S., Kuszewski, J., Nigles, M., Pannu, N. S., Read, R. J., Rice, L. M., Simonson, T., and Warren, G. L. (1998) *Acta Crystallogr., Sect. D54*, 905−921.
28. Brünger, A. T. (1992) *X-PLOR, version 3.1*, Yale University Press, New Haven, CT.
29. Collaborative Computational Project Number 4. (1994) *Acta Crystallogr. D50*, 760−763.
30. Laskowski, R. A., MacArthur, M. W., Moss, D. S., and Thornton, J. M. (1993) *J. Appl. Crystallogr. 26*, 283−291.
31. Thompson, J. D., Higgins, D. G., and Gibson, T. J. (1994) *Nucleic Acids Res. 22*, 4673−4680.
32. Hutchinson, E. G., and Thornton, J. M. (1996) *Protein Sci. 5*, 212−220.
33. Jones, T. A., Zou, J.-Y., Cowan, S. W., and Kjeldgaard, M. (1991) *Acta Crystallogr. A47*, 110−119.
34. Esnouf, R. M. (1997) *J. Mol. Graphics 15*, 133−138.
35. Rossmann, M. G., Liljas, A., Branden, C.-I., and Banaszak, L. J. (1975) in *The Enzymes* (Boyer, P. D., Ed.) pp 61−102, Academic Press, New York.
36. Kutzenko, A. S., Lamzin, V. S., and Popov, V. O. (1998) *FEBS Lett. 423*, 105−109.
37. Baker, P. J., Sawa, Y., Shibata, H., Sedelnikova, S. E., and Rice, D. W. (1998) *Nat. Struct. Biol. 5*, 561−567.
38. Liu, Z.-J., Sun, Y.-J., Rose, J., Chung, V.-J., Hsiao, C.-D., Chang, W. R., Kuo, I., Perozich, J., Lindahl, R., Hempel, J., and Wang, B. C. (1997) *Nat. Struct. Biol. 4*, 317−326.
39. Bertrand, J. A., Auger, G., Fanchon, E., Martin, L., Blanot, D., van Heijenoort, J., and Dideberg, O. (1997) *EMBO J. 16*, 3416−3425.
40. Jones, S., and Thorton, J. M. (1995) *Prog. Biophys. Mol. Biol. 63*, 31−65.
41. Holm, L., and Sander, C. (1993) *J. Mol. Biol. 233*, 123−138.
42. Barycki, J. J., O'Brien, L. K., Bratt, J. M., Rongguang, Z., Sanishvili, R., Strauss, A. W., and Banaszak, L. J. (1999) *Biochemistry 38*, 5786−5798.
43. Adams, M. J., Ellis, G. H., Gover, S., Naylor, C. E., and Phillips, C. (1994) *Structure 2*, 651−668.
44. Zhang, L., Chooback, L., and Cook, P. F. (1999) *Biochemistry 38*, 11231−11238.
45. Thoden, J. B., Frey, P. A., and Holden, H. M. (1996) *Biochemistry 35*, 5137−5144.
46. Perozich, J., Nicholas, H., Lindahl, R., and Hempel, J. (1999) in *Enzymology and Molecular Biology of Carbonyl Metabolism 7* (Weiner, H., Maser, E., Crabb, D. W., and Lindahl R., Eds.) pp 1−7, Kluwer Academic/Plenum Publishers, New York.
47. Jörnvall, H., Persson, B., Krook, M., Atrian, S., Gonzàlez-Duarte, R., Jeffery, J., and Ghosh, D. (1995) *Biochemistry 34*, 6003−6013.
48. Oppenheimer, N. J., and Handlon, A. L. (1992) *Enzymes (3rd Ed.) 20*, 453−505.
49. Soukri, A., Mougin, A., Corbier, C., Wonacott, A., Branlant, C., and Branlant, G. (1989) *Biochemistry 28*, 2586−2592.

BI000181H